Trans Indian Inst Met
https://doi.org/10.1007/s12666-024-03304-0

ORIGINAL ARTICLE

Artificial Slags with Modulated Properties for Controlled Nickel Dissolution in Smelting Process

Erdenebold Urtnasan[1,2] · Avneesh Kumar[3] · Jei-Pil Wang[4]

Received: 24 October 2023 / Accepted: 11 March 2024

Abstract In pyrometallurgy process involving drying, calcination and reductive smelting steps, Saprolite ore is subjected in an electric arc furnace to produce Fe–Ni alloy and Ni matte. To optimize the nickel smelting step, the slag consisted of MgO–SiO_2–FeO and having a lower viscosity and high fluidity is required. In this study, a number of new slag samples with varied degree of compositions are manufactured and used to examine the effect of their viscosity on nickel dissolution. Further correlation between the slag basicity and FeO addition on the smelting was also tested and simulated using Fe–Ni alloy from saprolite ore. As per the observations, the nickel dissolution increases with the increased content of FeO at a certain degree of activity which in turn can cause oxidation of nickel during the process. The slags with the ratio of $MgO/SiO_2 = 0.4–0.6$, 30% fraction of FeO, and a viscosity of 1.8–1.06 poise in the olivine zone are found effective for the lowest dissolution rate of nickel with 0.021, 0.022, and 0.018 wt.%. The lowest dissolution rate is recorded for the slag with MgO/SiO_2 ratio about 0.6. These slags with controlled amount of constituents could be used to recover precious metal from nickel smelter at a lower dissolution rate and thereby allowing to reduce the waste of the metal during smelting process.

Keywords Laterite deposits · Nickel dissolution processes · Fe–Ni alloys · Pre-melted slags · Physical and chemical properties of slag

1 Introduction

In recent years, the global consumption of nickel has been growing rapidly as it has been in demand for developing the electrical technology such as batteries and other products of stainless steel. Being now one of the most widely used metals, about 65% nickel is used for producing stainless steel whereas the rest (12, 8 and 5%) is consumed for manufacturing its super or non-ferrous alloys, electroplating and for batteries or other chemical derivatives, respectively [1, 2]. The natural and major deposit sources of nickel are laterite and magmatic sulfide. The laterite sulfide deposits represent about 70% of the nickel resources and are divided into the layers with different minerals, for example, limonite, saprolite and transition ores [3–7]. As an upper layer, the limonite ore has a lower grade of nickel (0.8–1.5%) and magnesium, silicon (0.5–1.5%) as compared to its counterpart saprolite. Currently, the limonite ore is processed by widely used methods known as hydrometallurgy, high-pressure acid leaching (HPAL—at high temperatures roughly 255 °C) and atmospheric pressure leaching (APL) [8]. In addition to this, a lower grade transition metals containing ore is treated by following hydrometallurgy method and a set of combined

Supplementary Information The online version contains supplementary material available at https://doi.org/10.1007/s12666-024-03304-0.

✉ Erdenebold Urtnasan
erdenebold@stda.edu.mn

✉ Jei-Pil Wang
jeipil.wang@gmail.com

1 Industrial Science Technology Research Center, Pukyong National University, Busan 48513, Republic of Korea

2 Darkhan School of Technology, Mongolian University of Science and Technology, Darkhan City, Mongolia

3 Department of Industrial Chemistry and CECS Core Research Institute, Pukyong National University, Busan 48513, Republic of Korea

4 Department of Metallurgical Engineering, School of Engineering, Pukyong National University, Busan 608-739, Korea

Published online: 15 April 2024

processes including pyro-hydrometallurgical, Caron and APL/HAPL [6, 9]. Contrary to limonite, saprolite ore contains a high composition of nickel and magnesium–silicon up to 1.8–3.0% and 15–35%, respectively [10, 11]. From this, Fe–Ni alloy can be produced upon subjecting the ore to pyrometallurgical process which involves consecutive steps (1) drying, (2) calcination, and (3) reductive smelting in an electric arc furnace subsequently [12]. However, the pyrometallurgical procedure can pose major disadvantages, for instance, during the drying step, about 30–40% moisture can be removed that leads to the consumption of a large amount of energy for calcination and generation of slag and thereby reducing the extraction of metals. Nevertheless, the pyrometallurgical method can be made convenient if nickel content in the ore is about 1.5% and about 90% metal recovery rate is achieved during production [13, 14]. In a report, a pyro-physical method combining reduction roasting and magnetic separation to recover the nickel from saprolite ore has been shown to have consumed lesser energy. However, the recovery rate of 90% could not be still accomplished [15, 16]. In another conventional processing technique, the roasted ore was made to undergo reductive smelting in order to obtain as high as 95% nickel recovery rate along with the production of nickel–iron alloy (20–70% Ni) as used in stainless steel [9]. It must be noted that the structural features and composition of MgO–SiO_2–FeO slag systems can influence the nickel loss and energy consumption during smelting, the slag also determines the gaseous motion, transportation of metal droplets, exchange of heat or electricity generated at the interface of separated metal and slag. From other studies, it is understood that in order to improve the transportation of mass and heat through the interface, the slag must have a lower viscosity that can further contribute towards a better solubility slag constituents or additives, and an effective metal separation from the treated slag phases [17]. Since the viscosity also is directly linked with the structure and chemical composition of the slag at a given temperature, a slag system with the lower viscosity and good fluidity is required for smelting process and extracting a higher amount of metal. Here in this study, we proposed new artificially prepared slag systems with the optimized composition and thereof structure and that are suitable for nickel smelting processes in industry. Scheme 1 shows the artificial slag developed in laboratory to have an optimized viscosity, compositions, and structure that are necessary for improved smelting process and recovering the transition metal. Further investigations with regard to the slag viscosity and its correlation with MgO–SiO_2 ratio and FeO were conducted to understand the dissolution rate of nickel from Fe–Ni alloy. For a simulated version of smelting process with saprolite ore, further theoretical analysis of viscosity as a function of MgO–SiO_2 ratio and FeO was also carried out to examine the dissolution of nickel into slag from Fe–Ni alloy. Our results have suggested that the slag systems with modulated properties reported here can be used to recover metal and thereby reducing waste metal content in the environment after smelting process.

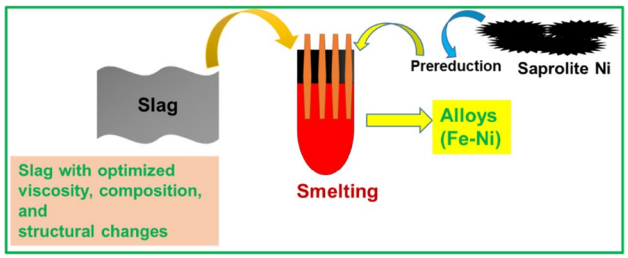

Scheme 1 Artificially designed and developed slag systems with optimized viscosity, compositions, and structure that can affect the smelting process of saprolite ore in industry and allow a cost effective recovery of metal with low energy consumption, and as a result preventing metal particles from going into the waste where they can be environmentally hazardous

2 Materials and Methods

2.1 Experimental Materials

The oxides used to prepare different slags in this study were purchased from Junsei Chemical Co. Ltd, Japan. The homogenous slags with different composition of MgO, SiO_2 and FeO as mentioned in Table 1 were prepared by mixing the respective oxide according to the $M/S = 0.2 - 0.8$ ratio and a desired quantity of FeO. Similarly, in a plastic vial, the Fe–Ni alloy was prepared by mixing a 80% Fe (99.9% pure iron powder) and 20% Ni (99.8% pure nickel powder) in a ratio of 8:2. For smelting test, a ratio of 100 g metal:100 g slag was maintained.

2.2 Experimental Apparatus

The smelting experiments were carried out in a Super Kanthal vertical tube furnace (impervious recrystallized magnesium oxide, 70 mm inner diameter) heated by molybdenum silicide ($MoSi_2$) elements at 1550 °C (Fig. 1). The Super Kanthal tube furnace is a vertical tube consisted of a furnace controller, a heating box with a B type thermocouple and vertical alumina tube with 75 mm diameter and 600 mm length. The Kanthal tube furnace can heat the sample to a maximum temperature of 1800 °C and can be sealed to avoid infiltration by air. A controlled flow of argon, nitrogen, carbon monoxide can be supplied to the furnace for the experiment. The operational temperature was monitored by a C type thermocouple (error of less than ± 0.5% °C) attached to the furnace center zone. The

Table 1 Different slags systems containing varied fraction of oxides prior to smelting process

Oxides	Wt. %										
Sample	M1	M2	M3	M4	M5	M6	M7	F8	F9	F10	F11
Ratio	0.2	0.3	0.4	0.5	0.6	0.7	0.8	0.6	0.6	0.6	0.6
MgO	11.67	16.15	20	23.33	26.25	28.82	31.11	30	26.25	22.5	18.75
SiO_2	58.33	53.85	50	46.67	43.75	41.18	38.89	50	43.78	37.5	31.25
FeO	30	30	30	30	30	30	30	20	30	40	50

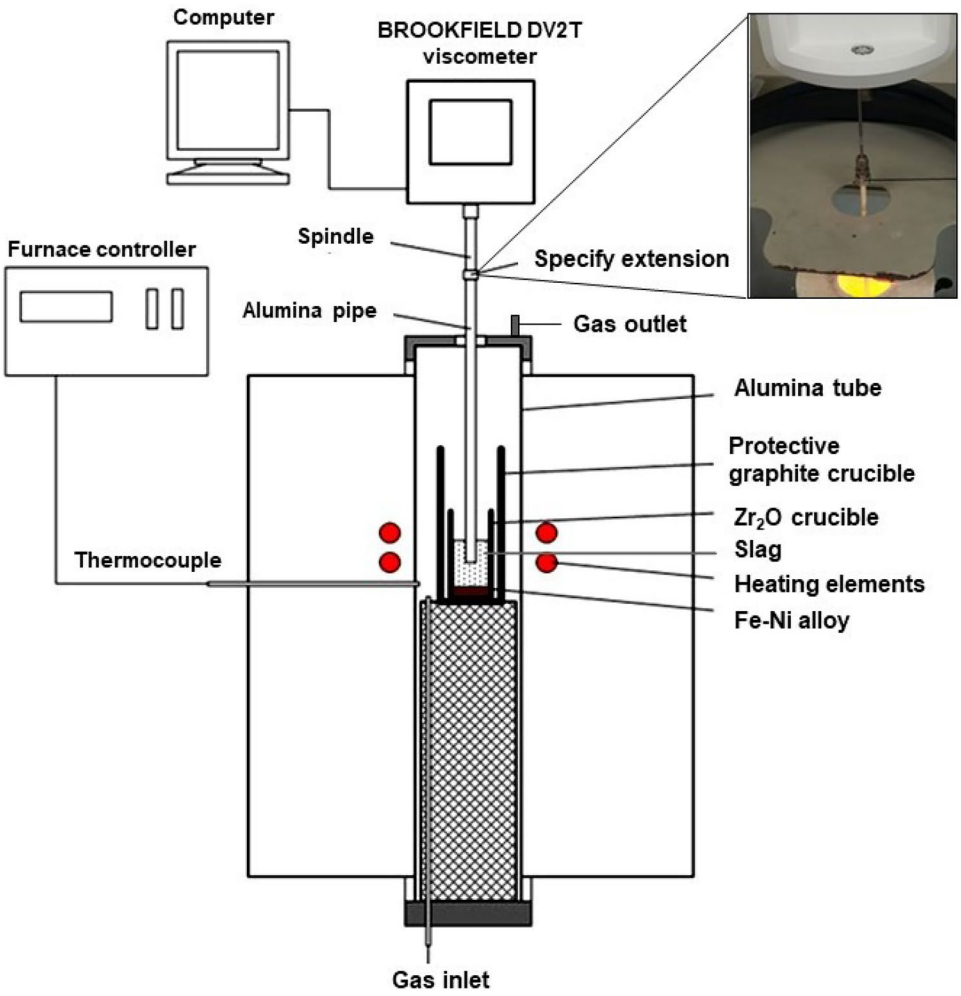

Fig. 1 Schematic diagram of experimental apparatus for testing the slags in smelting process and simultaneous measuring the viscosity of them

furnace is equipped with a temperature controlling system and programmable segments for precise control of heating rate, cooling rate, holding and time setting. An over-temperature controller and alarm are also mounted in the furnace for a continuous operation without the need of an attendant. The experimental gases for low oxygen partial pressure based on the CO/CO_2 ratio, and controlled by a mass flow controller (MFC), were injected from the bottom of the furnace through a working tube and supplied at a flow rate of 250 cc/min, with a mixture of CO gas adjusted at 200 cc/min, ± 2 cc, and the CO_2 gas at 50 cc/min, ± 0.5 cc.

A model of Brookfield digital viscometer DV2T with rotating cylinder mode was used in this study for measuring the viscosity of the slag. This viscometer was fixed on the super Kanthal vertical tube furnace as shown in Fig. 1. A LV4 type of spindle linked with an alumina rod in viscometer was 400 mm long and 6 mm in diameter, respectively. Prior to measuring the viscosity of the given slag, the viscometer was leveled and adjusted by using the two screws and stabilizing the bubble in the center of the circle. Afterward, the rotating spindle (speed 5–25 rpm) was lowered into the slag sample. The rotation of spindle allowed alumina rod to get immersed into the carbon crucible filled with

the slag as deep as 3 mm. To record the signal, the DV2T viscometer was connected to a computer with a Brookfield Rheocalc T software. At the end of experiment, viscosity was calculated by estimating the torque based on the selected LV4 spindle and speed rotation (ranging from 5 to 25 rpm).

2.3 Experimental Procedures

For the experimental process, MgO and SiO_2 powder oxides mixed at a ratio of = 0.2 − 0.8 and 20–50% FeO powder were placed on a prepared Fe–Ni alloy at a ratio of 1:1 in the ZrO_2 crucible with a diameter of 50 mm. Ar gas with CO/CO_2 was injected to remove oxygen in the environment at a rate of 300 cc/min for the smelting process. Also, experimental gases of the CO/CO_2 were supplied at a flow rate of 250 cc/min. The temperature was heated at a rate of 5 °C/min and then cooled at a rate of 5 °C/min after holding for 20 h. The slag was removed from the crucible and cooled in the air. The slag samples were analyzed using X-ray fluorescence (XRF) and X-ray Diffraction (XRD) analysis, and an inductively coupled plasma-mass spectrometer (ICP-MS) was used out to determine the content of nickel in the slag. All analyses were conducted in the Lab collaboration center of Pukyong National University, Korea. XRF spectrometer was a Shimadzu XRF-1700 X-ray fluorescence spectrometer. The sample was placed inside a platinum crucible and loaded into an XRF machine, wherein XRF machine, the beam was loaded into the sample holder, after which, the sample was ionised by x-rays under vacuum medium. Then, fluorescent x-rays were analyzed and compared with certified references and calculated by XRF OXSAS software. X-ray diffractometer was a model of Rigaku UltimaIV that has the 3 kW Cu-Kα X-ray tube; XRD analysis was conducted with 2θ degree in the range from 10° to 80° using Cu Kα radiation at 30 kV and 10 mA. The step size was set at 0.2° within 0.6 s. The detected data as the X-ray signal were converted to a count rate. The ICP-MS spectrometer was a PerkinElmer NexION 300D Inductively Coupled Plasma–Mass Spectrometry. ICP-MS analysis is a sensitive method for detection and confirmation of metal ions with a higher liner dynamic range. Samples were placed in the sample introduction system, creating a fine aerosol that is subsequently transferred to the argon plasma. The high-temperature plasma atomises and ionizes the sample, generating ions, which are then extracted through the interface region and into a set of electrostatic lenses. The ion optics focuses and guides the ion beam into the quadrupole mass analyzer. The mass analyzer separates ions according to their mass–charge ratio (m/z), and these ions are measured at the detector.

During measuring viscosity of the slag, the ZrO_2 containing the Fe–Ni alloy and pre-melted slag with 200 g by a ratio of 1:1 was placed in even temperature zone of the vertical tube furnace. The experimental temperature was maintained at 1550 ℃ for 20 h with a heating rate of 5 ℃/min. The LV4 spindle linked with an alumina rod was used to measure viscosity; it drove to raise or lower with DV2T viscometer using screw mechanism and immersed about 3 mm into molten slag. Five rotation rates varying from 5 to 25 rpm with step of 5 rpm were used for 5 min. The viscometer was calibrated by Brookfield standard 5000 liquid with 5040 cP at a room temperature of 25℃.

3 Results and Discussion

As described earlier, the viscosity is one of the most important thermo-physical properties of metallurgical slag. The fluctuations in viscosity mainly depend on the structure and chemical composition of the slag at a given temperature. A slag with low viscosity is desirable for controlling the transfer of mass and heat while separating the metal in smelting process [18]. In other terms, the viscosity can also reflect the fluid's internal resistance to flow and might be considered as an indicator of fluid friction. Determining the viscosity of slag is a difficult task due to its composition and multi-component chemical system. However, previously a method known as viscosity approximation has been applied to estimate the same by obtaining the optical basicity of the slag at a given temperature and using an empirical equation [19]. The equation formulated with the optical basicity is as follows:

$$\ln\eta = \frac{1}{(0.15 - 0.44\Lambda)} - \frac{1.77 + 2.88\Lambda^{-1}}{T} \tag{1}$$

where η = viscosity, Poise [P], Λ = optical basicity, T-temperature, K.

$$\Lambda = \frac{\sum x_1 n_1 \Lambda_{th1} + x_2 n_2 \Lambda_{th2} + \cdots}{\sum x_1 n_1 + x_2 n_2 + \cdots} \tag{2}$$

Here, Λ_{th2} represents the optical basicity value of the individual component, x_i-mole fraction of component 'i' in the slag, and n_1 denotes compositional fraction.

Several other mathematical models have been also proposed for estimating the viscosity of the slag based on its chemical composition at a given temperature. Among them, Riboud and Urbain models are found the most effective to describe the viscosity of the slag by applying the Weymann equation [19–21]. According to these models, the following equation has been defined:

$$\eta = AT\exp\left(\frac{B}{T}\right) \tag{3}$$

where A and B parameters describe the functions of slag composition expressed in cumulative molar fraction by using Eqs. 4 and 5.

$$A = \exp\left(-17.51 + 1.73X_{CaO} + 5.82X_{CaF_2} + 7.02X_{Na_2O} - 33.76X_{Al_2O_3}\right) \quad (4)$$

$$A = \exp\left(31140 - 23896X_{CaO} - 46356X_{CaF_2} - 39159X_{Na_2O} + 68833X_{Al_2O_3}\right) \quad (5)$$

X-ray fluorescence (XRF) based on wavelength-dispersive spectroscopic principles is well suited for bulk chemical analyses of major and trace elements within a large amount of the sample. Hence, the chemical composition of the bulk slags reported here was determined by XRF to further evaluate the M/S ratio and fraction of FeO additives. The results are shown in Table 2. The XRF results have revealed a lower MgO/SiO_2 ratio for S1, S2 and S3 slags as compared to their initial composition used during physical mixing, for M1, M2 and M3. Also, the SiO_2 content in slag was found to be higher than the estimated value. It might have changed due to the role of SiO_2, because slags are compounds associated with silicate compounds. Ni content in the slag was not measured in XRF analysis, which could indicate low amount of dissolved nickel.

In principle, optical basicity (Λ) represents the degree of acid–base nature of a nonaqueous and nonprotonic chemical systems such as binary oxides, silicates, and melts. It can provide the information about the complexation of metal ions in a framework. By using these slags in smelting nickel experiments at 1550 °C, the optical basicity and viscosity of the applied slags were calculated simultaneously as a function of chemical composition of the pre-melted slag (Fig. 2). It was observed that the optical basicity of the slag increases with a higher M/S ratio and MgO content in the slag. However, with a lower content of FeO (20 wt.%), the optical basicity decreases to 0.69 (Fig. 2). A strange behavior in optical basicity occurs when the content of FeO was varied from 30 to 50 wt.%. Unexpectedly, it has increased with a higher content of FeO. It can be inferred that the viscosity has shown a direct dependence on the slag basicity (Fig. 2). Furthermore, the viscosity of the slag declined as its basicity increased with an exception where for 20 wt.% FeO, it

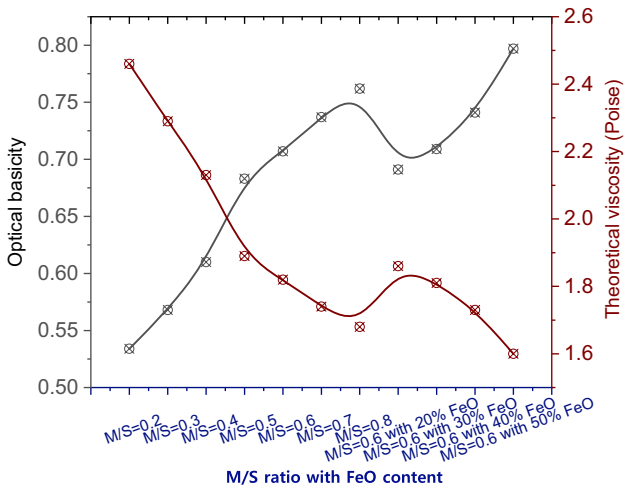

Fig. 2 Effect and correlation of MgO/SiO_2 ratio with FeO on optical basicity and theoretical viscosity of the slags prepared for smelting process

further increased to 1.86 Poise with a low degree of basicity. Obviously, the viscosity and optical basicity of the slags are interconnected and can give some insights about the fluidity or friction resistance in the slag.

Inductively coupled plasma-mass spectroscopy (ICP-MS) is a reliable technique used to identify atomic composition of a complex sample and detect even a small trace of any element. During smelting process, the slags may have a small nickel content, and therefore, ICP-MS was used to map the presence of nickel atoms in the system (Fig. 3). Smelting experiments using the slag S5 ($M/S = 0.2$–0.8, 20–50% FeO) were conducted together with Fe–Ni alloy at 1550 °C for 24 h to monitor the nickel dissolution and trace the metal content thereafter. The outcome of ICP-MS tests of the slags having metal atoms dissolved within during smelting is shown in Fig. 3. It can be seen that the nickel trace was up to 0.017 wt.% initially for 10 h after smelting process began. For next 10 h of smelting, the nickel content did go beyond 0.0178 wt. %.

It is clear that the slag has shown a low dissolution toward the nickel particles produced during the smelting process. The viscosity by DV2T viscometer measurements has also indicated the dependence of slag viscosity on its basicity as shown in Fig. 4a. With the basicity of 0.8, the slag viscosity

Table 2 Oxides and composition of slags prior to smelting as analyzed by XRF

Oxide	Wt. %										
Sample	S1	S2	S3	S4	S5	S6	S7	N8	N9	N10	N11
Ratio	0.16	0.26	0.37	0.52	0.61	0.71	0.81	0.62	0.60	0.59	0.60
MgO	10.31	15.48	20.07	24.51	27.51	29.83	32.34	30.91	26.86	23.23	19.44
SiO_2	64.74	59.13	54.99	46.60	45.08	42.12	39.92	49.89	44.29	38.85	31.95
FeO	25.02	24.61	24.94	28.23	27.41	28.05	27.74	19.02	28.15	37.35	48.21

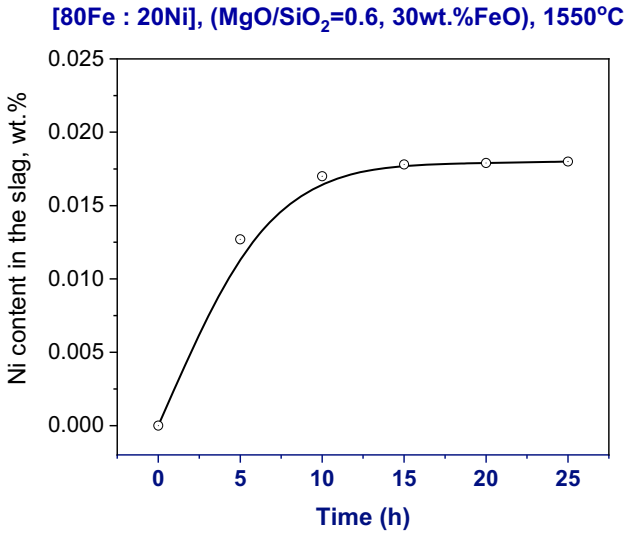

Fig. 3 Ni distribution on the holding time of pre-melted slag of S5 at 1550 °C

decreased further to a minimum level of 0.6 poise. With respect to the nickel content, it was found to be 0.027 wt.% with a M/S ratio of 0.2, however began to decrease to 0.024, 0.019, and 0.0185 wt.% upon lowering the ratio of M/S to 0.3, 0.4 and 0.5, respectively. The lowest Ni content about 0.0145 wt.% was recorded with the ratio 0.6. Furthermore, an increment in Ni content to 0.027 and 0.037 wt.% with the increased amount of MgO and SiO_2 (0.7–0.8) was also seen confirming that Ni content dissolution in slag occurred even after decreasing its viscosity. Further experiments with the addition of 20% FeO, the Ni content in the slag was estimated to be 0.0175 wt.% at a 0.6 ratio of MgO/SiO_2 (Fig. 4b). It is interesting to note that upon increasing FeO (from 30 to 50%) the Ni content in the slag also rose to 0.018, 0.025 and 0.043 wt.%, respectively. The outcome has shown an inverse relationship between the viscosity of the slag and the dissolution of nickel in it.

To understand the structure of our ternary system composed of $MgO–SiO_2–FeO$ and its correlation with the viscosity, the Factsage 8.2 (FToxid database) software was applied (Fig. 5). As per the results, the slag with M/S ratios of 0.2–0.4 exhibited a dominance in silicon oxide zone estimated for $FeO–SiO_2$ system. However, the slags S5 to N11 appeared in the olivine $2(Mg,Fe)O{\cdot}SiO_2$ zone upon the addition of FeO (20 wt. %) and a M/S ratio of 0.6. The slags with 20 wt. % FeO and M/S ratio of 0.6 had a boundary with the olivine and magnesium silicate area. As shown in the diagram of $MgO–SiO_2–FeO$ ternary system, the slags are presented in different zones depending on the M/S ratio and melting temperature. At 1600 °C, the M/S ratio for S1–S3 slag was 0.2–0.4, while it increased to 0.5 (S4 slag) when the temperature was decreased to 1500 °C. However, when the M/S ratio for S5–S8 increased to 0.6–0.8, the slag temperature increased again. With further addition of FeO (40 and 50 wt.%), the structure of slag has shown a shift towards the iron monoxide zone. The viscosity of the slag in the silicon oxide zone was relatively as high as 1.8–6 poise, whereas in the olivine zone it decreased to 0.6 poise. However, when the FeO content in the slag increased from 20 to 50 wt.%, the slag structure existed in the zone of olivine, where there is the viscosity of slag decreased from 0.5 to 0.2 poise. In addition, the slag temperature of N10 and N11 samples in olivine zone is expected to decrease below 1500 °C, which is consistent with the decrease in the slag viscosity.

Further to analyze the structure of the slag upon cooling and heating, X-ray diffraction analysis (XRD) experiments were conducted to have an insight about the crystalline domains in the slag and their relationship with the composition (Fig. 6). During cooling cycle, the slow rate of cooling can allow the slag to crystalize [22]. The $MgO–SiO_2–FeO$ slag system displayed glassy non-crystalline regions due to

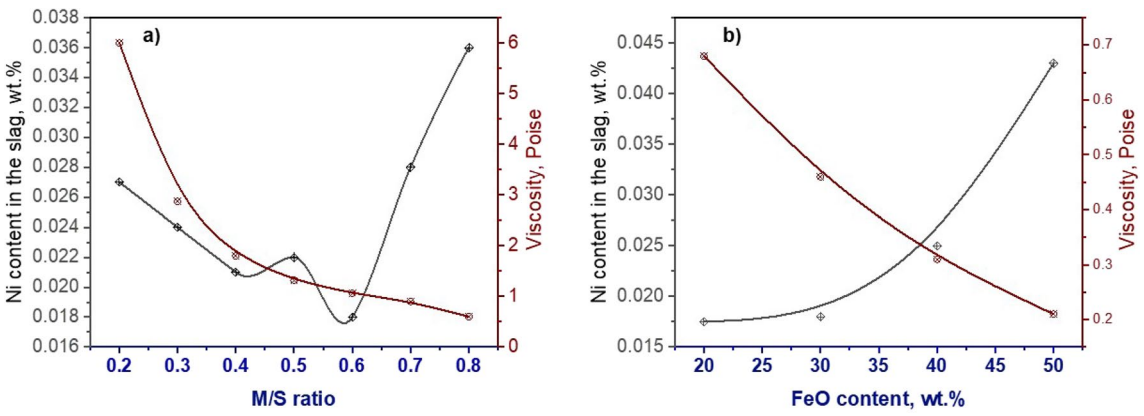

Fig. 4 Relationship between Ni distribution and slag viscosity associated with the **a** MgO/SiO_2 ratio and **b** FeO and Ni content of the pre-melted slag at 1550 °C

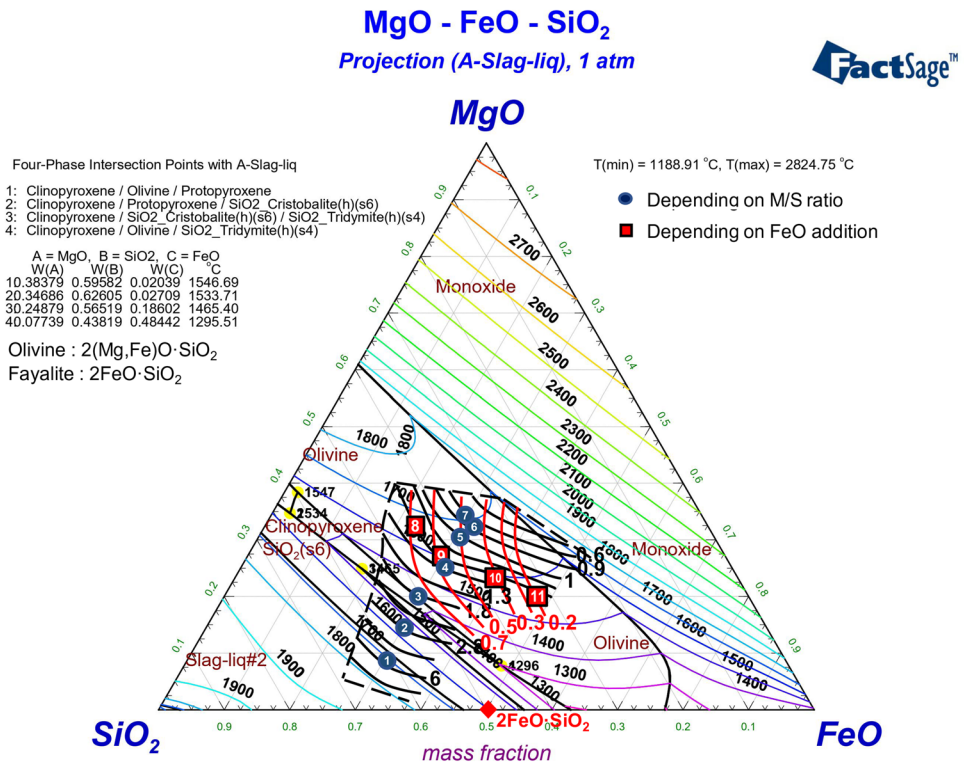

Fig. 5 Determination of the viscosities (in poise) of MgO–FeO–SiO_2 system slag depending on *M/S* ratio and FeO content by using FactSage 8.2 FToxid database

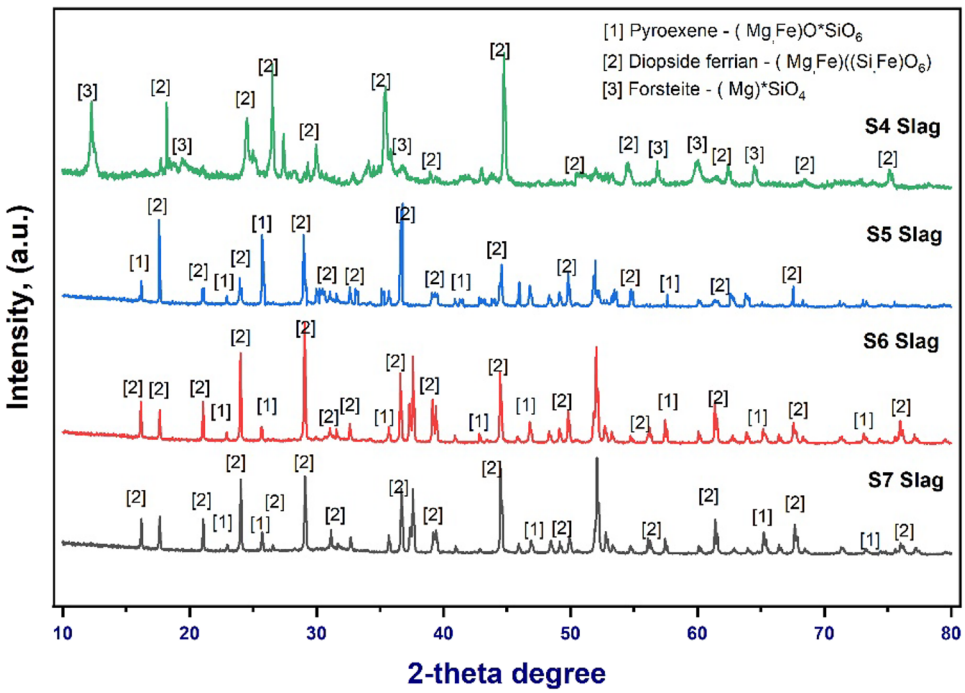

Fig. 6 XRD patterns of the pre-melted slag of S4 to S7 after heating at 1550 °C for 20 h and cooling thereafter recorded at room temperature

a high SiO_2 content. From the crystalline phase appeared in XRD pattern, the mineralogical composition of pre-melted slag was also estimated. In a slag (S4) with a *M/S* ratio of 0.5 and 30% FeO, a diopside ferrian phase prevailed particularly in the olivine zone (Fig. 6). The olivine zone is represented by 2(Mg, Fe)O·SiO_2 structure in which several metals such as Ca, Fe, Mn, Ni, and Mg can exist [23]. A small degree of forsteite phases was also mapped and was associated with the MgO–SiO_2 complex containing a high fraction of silicon. The slags S5 to S7 were mainly dominated by diopside

phase along with few pyroexene phases. Also, FeO and MgO oxides were formed as a result of lesser SiO_2 content in the slags. With a M/S ratio of 0.5 and relatively high SiO_2 content, the various combined phases such as Mg_2SiO_4 existed in the slag. It is suggested that in the process of cooling the slag from its molten state, different types of compounds might phase separate from homogenous slag, and the resulted complex can be enriched by more SiO_2 to form new silicate phases, and thereby affecting the crystalline nature of the slag. The results of XRD analysis proved that the premelted slag has an olivine structure in a molten state. The XRD data show the presence of major compounds namely magnesium silicates, 2(Mg, Fe)O•SiO_2 magnesium, and iron silicates in the slag made up of MgO–SiO_2–FeO ternary system.

The simulated smelting experiments of Fe–Ni alloy under the MgO–SiO_2–FeO slag system were conducted at 1550 °C for 20 h. The correlation between basicity and viscosity according to the M/S = 0.2–0.8 ratio and FeO content in the slag was studied successfully in order to achieve a low dissolution of nickel into slag and subsequently for obtaining a high recovery rate of nickel during smelting process. The redox reactions between the metals in the salg were investigated to better understand the nickle dissolution. Oxidation of iron and nickel and within Fe–Ni alloy can be expressed by Eq. 6, as the equations indicate that the nickel content in the slag is directly related to the free oxygen. With the amount of free oxygen, the nickel content in the slag may also tend to increase.

$$Me^{2+}_{(liq)} + \frac{1}{2}O_{2(gas)} + O^{2-}_{(liq)} = MeO^{2-}_{(liq)} \quad (6)$$

As shown in Eq. 6, the nickel content in slag depends on the oxygen partial pressure of the furnace atmosphere and the activity of the O^{2-} ions in the slag [24]. From Eq. 6, the equilibrium constant (K) can be expressed as following Eq. 7:

$$K = \frac{a_{(MeO)}}{a_{[Me]} \cdot p(O_2)^{\frac{1}{2}}} \quad (7)$$

where a_i describes the activity of composition i, $p(O_2)$–oxygen partial pressure.

Thermodynamic modeling considers the stable phase and phase composition belonging to the initial and final states of a given system, where the calculation has been focused on two properties such as enthalpies and Gibbs free energies of system. In thermodynamic analysis, $\Delta G > 0$ indicates that a chemical reaction is not possible to occur; if $\Delta G < 0$ and with more negative value, the chemical reaction can spontaneously and intensively occur. The oxidation behavior of nickel and other compounds of the slag produced during the nickel smelting process was also examined by thermodynamic analysis carried out using a Factsage 8.2 FactPS and FToxid database. According to the changes in Gibbs energy for each component including Ni, it can be said that the nickel oxidizes rapidly as compared to other thermodynamically stable compounds generated in slag at a given temperature (Fig. 7a). The thermodynamic analysis of the slag was in agreement with smelting experimental results and have concluded that with a higher amount of FeO the nickel can react with the oxygen rapidly.

In order to properly evaluate the compositional variation of the concentrate, and effect of composition on stability of

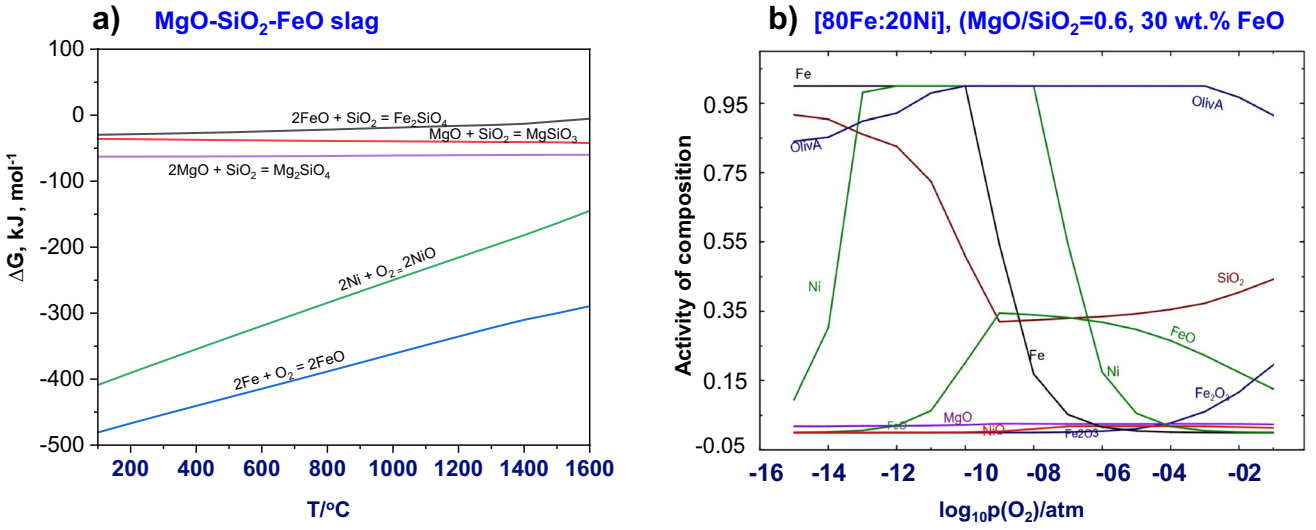

Fig. 7 Oxidation behavior of compositions in the slag and Fe–Ni alloy associated with the **a** temperature dependent Gibbs free energy changes in the components of the slag, **b** effect of oxygen partial pressure () on the activity of compositions in Fe–Ni alloy and MgO–SiO_2–FeO slag by Factsage 8.2 FToxid database

a particular end component during reaction, activity (a_i) of a component i, which is one of thermodynamic property, should be considered. Thermodynamic activity is value that indicates how reactive the particular end component is in a given material composition. Figure 7b shows the activity of the major compositions of Fe–Ni alloy and slag with MgO/SiO_2 = 0.6 ratio and 30 wt.% FeO at 1550 °C temperature as a function of the oxygen partial pressure based on thermodynamic calculations by Factsage 8.2 FToxid database. According to the diagram, the activity of the Fe and Ni in the Fe–Ni alloy is high when the oxygen partial pressure is − 8, but the activity of Fe and Ni decreases with increasing oxygen partial pressure from − 7. However, the activity of Fe_2O_3 and NiO in the slag increase. When the oxygen partial pressure increases above − 3, the activity of olivine decreases, but the activity SiO_2 increases. The increases in activity of Fe_2O_3 and SiO_2 indicate that the formation of the iron silicate in the slag occurs with an increase in the oxygen partial pressure.

4 Conclusions

The artificial slags composed of oxides, e.g., MgO, SiO_2, and FeO were prepared and analyzed in a simulated smelting process by using Fe–Ni alloy in order to prevent or lower Ni dissolution for recovering the metal that can be usually wasted in an industrial smelting process which generates a higher amount of the slag containing these precious metals. A correlation between the viscosity and basicity of the slags was made by conducting practical as well as theoretical experiments such as thermodynamic studies in which oxidation of nickel was found to be related with the content of FeO added during the experiment. At a temperature of 1600 °C, the oxidation of iron and nickel takes place rapidly as compared to other thermodynamically stable compounds formed during smelting. Theoretical calculations as well as experiments have suggested a decline in viscosity of the slag with its increasing basicity and FeO fraction. The nickel dissolution remained unaffected when the viscosity was decreased. However, with increasing content of FeO, the nickel dissolution occurred rapidly and was linked with the oxidation process involving nickel. It was observed that at a basicity of 0.6 the SiO_2 reacts with MgO quickly allowing the release of FeO which in turn oxidizes the nickel. The slags with a M/S = 0.4–0.6, 30% FeO and viscosity of 1.8–1.06 poise displayed crystalline domains in olivine zone. This crystalline slag (M/S = 0.6) has shown the lowest dissolution rate for nickel. These optimized slags reported here are the potential models for their usage in smelting process in which a high recovery of metal or alloy can be accomplished and further loss of precious metal to the environment can be prevented. In future, these optimized slags with tuned viscosity and basicity will be tested with the natural occurring nickel ores in order to extract a higher content of the desired metal which is in our case would be nickel alloy.

Acknowledgements This research was funded by Brain Pool program funded by Ministry of Science and ICT through the National Research Foundation of Korea (RS-2023-00222959).

Author contributions Erdenebold Urtnasan designed the research project, performed the experiments, carried out writing, Avneesh Kumar reviewed and edited; Jei-Pil Wang reviewed and checked the manuscript. All authors have read and agreed to the published version of the manuscript.

Declarations

Conflict of interest The authors declare no conflict of interest.

References

1. Yayat I. S, Iqbal. H.S, *Mater. Today. Proc* 13 (2019) 127. https://doi.org/10.1016/j.matpr.2019.03.201
2. Fajar N, Widi A, Fathan B, and Bambang S, *Mater. Today: Proc* **44** (2021) 1488. https://doi.org/10.1016/j.matpr.2020.11.687
3. Saeed F, Michel C, Simon BB, and Odile L. *J. Geochem. Explor* **196** (2019) 270. https://doi.org/10.1016/j.gexplo.2018.11.002
4. Asran I, Koki K, and Katsuaki K, *J. Geochem. Explor* **165** (2016) 174. https://doi.org/10.1016/j.gexplo.2016.03.002
5. Wei F, Yangyang F, Peng L, and Yongzhang Z, *Minerals* **51** (2019) 1. https://doi.org/10.3390/min9010051
6. Anne O, and Nic B, *Miner. Eng* **54** (2013) 2. https://doi.org/10.1016/j.mineng.2013.02.012
7. Séverine L, Emile B, Peter D. Erskine, and Antony Van D. E, *J. Geochem. Explor* 202 (2019) 113. https://doi.org/10.1016/j.gexplo.2019.03.011
8. Bo Li, Hua. W, and Yonggang W, *Miner. Eng* 24 (2011) 1556. https://doi.org/10.1016/j.mineng.2011.08.006
9. Norgate T, and Jahanshahi S, *Miner. Eng* **24** (2011) 698. https://doi.org/10.1016/j.mineng.2010.10.002
10. Kaczan W, Kudełko J, and Herbert W, *Miner. Econ* **34** (2021) 315. https://doi.org/10.1007/s13563-021-00269-0
11. Park J O, Hyun-Soo K, and Sung Mo J, *Miner. Eng* **71** (2015) 205. https://doi.org/10.1016/j.mineng.2014.11.011
12. Muhammad H U, and Leili T K, *Miner. Eng* **157** (2020) 106563. https://doi.org/10.1016/j.mineng.2020.106563
13. Hongyu T, Zhengqi G, Ruoning Z, and Liaoting P, *Powder Technol* **394** (2021) 120. https://doi.org/10.1016/j.powtec.2021.08.043

14. Keith Q, Jason N C, William S, and Addai-Mensah J, *Miner. Eng* **79** (2015) 269. https://doi.org/10.1016/j.mineng.2015.03.017
15. Ender K, *Metals* **9** (2019) 974. https://doi.org/10.3390/met9090974
16. Sadia I, and Rajiv R, S, and Rabia S. *Sep. Purif. Technol* **232** (2020) 115971. https://doi.org/10.1016/j.seppur.2019.115971
17. Wang Kun, Liu Yan, Hao Jun, Dou Zhi-he, and Zhang Ting-an, *Trans. Nonferrous Met. Soc. China* **33** (2023) 2511. https://doi.org/10.1016/S1003-6326(23)66277-6
18. Sinelnikov. V, and Kalisz. D, *Arch. Foundry Eng* 15 (2015) 119. https://bibliotekanauki.pl/articles/382452
19. Verlag Stahleisen GmbH. Slag atlas. 2nd edition, Germany, 1995, 350. ISBN: 3-514-00457-9.
20. Yao L, Shan R, Xiaoqing. W, and Jibin L, *Steel Res. Int* 87 (2016) 241. https://doi.org/10.1002/srin.201500021
21. Mills. K. C, Yuan. L, Jones R.T, Estimating the physical properties of slags. *J.South. Afr. Inst. Min. Metal*, 111, (2011). https://www.pyrometallurgy.co.za/Mintek/Files/2011Mills.pdf
22. Markssuel Teixeira Marvila, Afonso Rangel Garcez de Azevedo, and Carlos Mauri´cio Fontes Vieira. *J. Mater. Res. Technol* **23** (2023) 4551. https://doi.org/10.1016/j.jmrt.2023.02.088
23. George W. M, in: Micheal Fleischer, Data of Geochemistry, 6th edition, Washington, 1963, p 54–76.
24. Turkdogan. E.T, Fundamentals of steelmaking. The Institute of Materials 1. Carlton House Terrace London, 2010, 140 pp ISBN 9781906540975.